J Mater Sci (2010) 45:5171–5176
DOI 10.1007/s10853-010-4554-9

The influence of ECAP on the small punch creep of Al–4 vol.% Al_4C_3 composite

Ferdinand Dobeš · Karel Milička · Michal Besterci · Tibor Kvačkaj

Received: 15 January 2010 / Accepted: 16 April 2010 / Published online: 5 May 2010
© Springer Science+Business Media, LLC 2010

Abstract The creep behaviour of a composite based on an aluminium matrix reinforced by 4 vol.% Al_4C_3 was studied at temperatures of 623 and 723 K by small punch testing with a constant force. The composite was tested in two different states: (i) as received by mechanical alloying with hot extrusion (HE) as the final operation and (ii) with equal channel angular pressing (ECAP) superimposed on the hot-extruded material. The ECAP does not improve the observed creep resistance. The reduction of force leading to the same deflection rate is not very significant. This points out that the ECAP process of the present composite, which produces substantial strengthening at lower temperatures, is not accompanied by pronounced weakening of creep resistance at elevated temperatures. The threshold force in the ECAP material is about 5 N weaker than in the HE material.

Introduction

The mechanical properties of aluminium-based metal–matrix composites (MMCs) in combination with their relatively low density have made them attractive for numerous applications ranging from aerospace to sport accessories [1]. It is clear that the method chosen for processing the composite has a strong impact on the final quality of the material. The present scientific research is intensively focused on the formation of ultra-fine-grained structures (UFG with grain diameters in the range of 100 nm–1 μm) and nanoscale structures (NSG with grain diameters $\leq$ 100 nm) in polycrystalline metallic materials, attained by severe plastic deformation (SPD). UFG and NSG materials produced by SPD are characterized by increasing values of strength, elongation, fatigue properties and superplasticity. The resulting properties are dependent on the nanoscaled structure, its distribution in the material, texture and other microstructural properties. Various plastic deformation processes have been designed for processing materials using simple shear. One of these techniques is equal channel angular pressing (ECAP) [2–5]. The method involves pressing the material through a die containing two channels of equal cross-section. Shearing strain depends on the geometry of the ECAP instrument [5], which is defined by the angle between the two separate parts of the channel [6, 7], the angle on the outer corner of the die [8], the pressing speed [9, 10] and temperature [11], etc. The technique was applied mainly to easy-to-work materials like Al [12–15] and Cu [16]. The application to difficult-to-work materials like titanium alloys [17, 18] or magnesium alloys [19, 20] is still limited. Little information is currently available on the application of ECAP to MMCs [21–24].

As a rule, only laboratory-scale samples of ECAP products are available for subsequent testing. Moreover, since the ECAP process offers a large variety of parameters, the conventional testing of products is very material-consuming. From this point of view, miniaturized methods like small punch (SP) [25–27] may be promising for the

F. Dobeš (✉) · K. Milička
Institute of Physics of Materials, Academy of Science of the Czech Republic, Žižkova 22, 616 62 Brno, Czech Republic
e-mail: dobes@ipm.cz

M. Besterci
Institute of Materials Research of Slovak Academy of Sciences, Watsonova 47, 043 53 Košice, Slovak Republic

T. Kvačkaj
Department of Non-ferrous Metals and Waste Treatment, Faculty of Metallurgy, Technical University, Letná 9/A, 042 00 Košice, Slovak Republic

testing of ECAP products. The method uses small disc specimens up to 10 mm in diameter with thicknesses up to 0.5 mm. The specimen is placed on a ring, and a ball (or a punch with hemispherical tip) is forced into the centre of the specimen. In the present contribution, the SP testing is applied to an aluminium-based composite prepared by the ECAP procedure. The results are compared with the previously reported testing of the same composite prepared by the powder-metallurgy route with hot extrusion as the final operation (designated as HE in what follows) [28].

It is obvious that long-term high-temperature applications of ECAP materials are not expected due to the well-known reciprocal grain-size dependence of creep rate controlled by diffusional flows (Nabarro-Herring and Coble mechanism) [29]. Nevertheless, a knowledge of short-term behaviour at elevated temperatures is necessary in predicting the safety of constructions in response to certain accidents or particular service conditions.

Experimental

Experimental material was prepared by the powder-metallurgy route by the method of mechanical alloying. Aluminium powder with a particle size of <50 μm was dry milled in an attritor for 90 min with the addition of graphite KS 2.5 in an amount corresponding to 4 vol.% of Al_4C_3 in the resulting product. The mixture was then cold pressed using a stress of 600 MPa into compacts of cylindrical shape (40 mm in diameter). Subsequent heat treatment at 823 K for 3 h induced the chemical reaction $4Al + 3C = Al_4C_3$. The cylinders were then hot extruded at 873 K with a 94% reduction in cross-section into rods of 10 mm diameter. Due to the high affinity of Al to O_2, the system also contained a small amount of Al_2O_3 particles (ca. 1 vol.%). They were formed during the reaction milling in the attritor. The residual porosity of this material was less than 1 vol.%. The experimental material was produced in the Institute for Chemical Technology of Inorganic Materials, Technical University of Vienna.

Hot-extruded rods were processed by ECAP. ECAP was realized at room temperature by route C (sample rotation around the axis of about 180° after each pass), with two ECAP passes (sample sizes: diameter $D = 10$ mm and length $l = 80$ mm) and a 90° angle between the two channels.

The specimens for SP testing were prepared by cutting slices 1.2 mm thick and 8 mm in diameter using spark erosion. The slices were perpendicular to the longitudinal axis of ECAPed rods. The slices were ground carefully from both sides equally and finally polished to 1,200 grits. The final thickness of 0.500 ± 0.002 mm was measured by a micrometre with a resolution of 1 μm. The SP testing assembly is described in more details in our previous article [28]. The main dimensions are a lower die diameter of 4 mm and a punch diameter of 2.5 mm. The tests are performed in the constant force regime in a protective argon atmosphere.

The results of extensive microstructural characterization of the material under investigation can be found in previous articles [30, 31]. Grain size was determined by intercept length measurements (Saltykov method). Particle distribution was examined by means of quadrate count statistics and by polygonal method (the analysis of the Voronoi mosaic).

Results

Examples of the dependence of the central deflection versus time obtained in the SP test arrangement are given in Fig. 1. It can be seen that the same general features of the curve can be observed as in conventional creep tests for the material both without and with ECAP. It should be noted that the time to fracture in the ECAP material is substantially shorter.

The dependence of the minimum deflection rate on the applied force for two temperature levels is given in Fig. 2. The dependence can be described by a power-law relationship of the form:

$$\dot{\delta} = A_S \cdot F^{ns}, \quad (1)$$

where $\dot{\delta}$ is the minimum deflection rate, F the acting force and A_S a temperature-dependent constant. The deflection

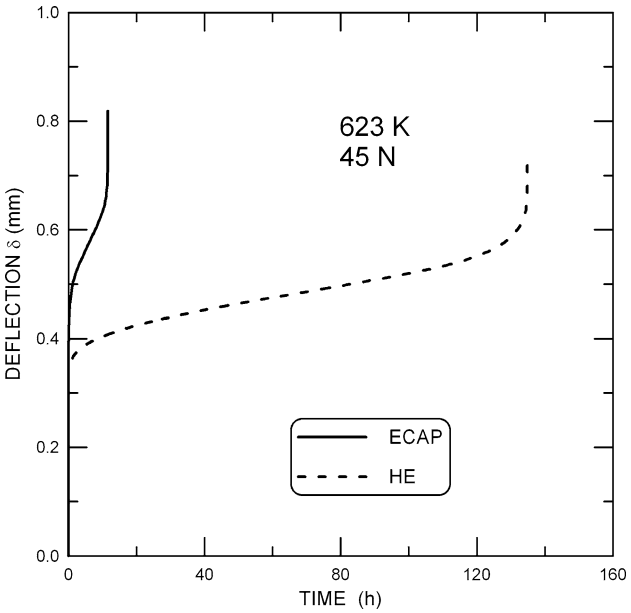

Fig. 1 Example of the time dependence of the measured central deflection

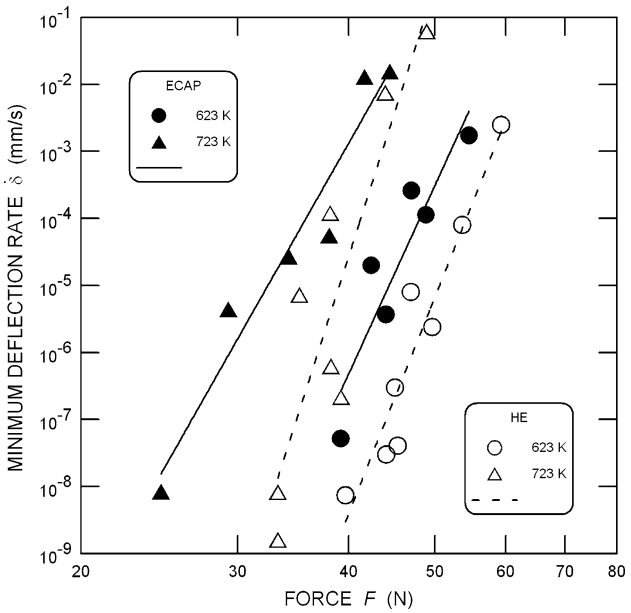

Fig. 2 Dependence of the minimum deflection rate on the applied force

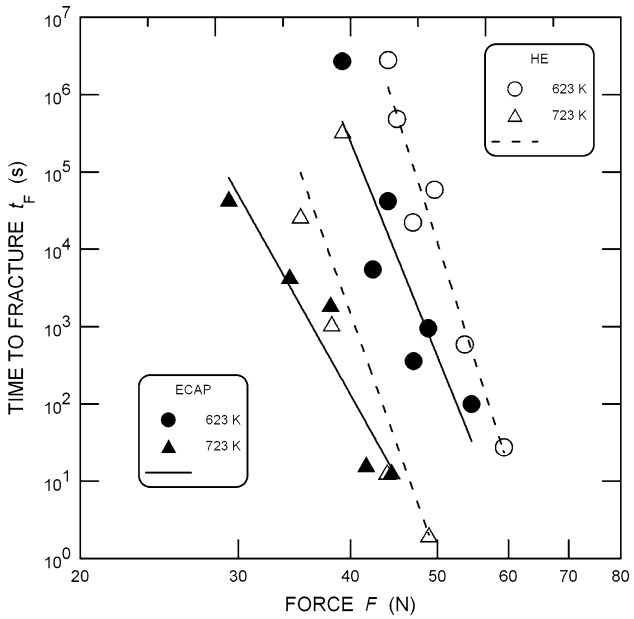

Fig. 3 Dependence of the time to fracture on the applied force

rate in the ECAP state is about two orders of magnitude faster than in the state not subjected to ECAP (64 times at 623 K; the exact value at 723 K is dependent on the applied force). The values of the exponent n_S after HE, as reported previously [19], are 33 at 623 K and 41 at 723 K, respectively, and they are slightly lower after the ECAP process: 29 at 623 K and 23 at 723 K. The high values of the exponent n_S indicate that the deformation is controlled by the same mechanism in both HE and ECAP composite. The reduction of force leading to the same deflection rate is not very significant. This points out that the ECAP process, which produces substantial strengthening at lower temperatures, is not accompanied by pronounced weakening of creep resistance at elevated temperatures.

The dependence of the time to fracture, t_F on the applied force F is given in Fig. 3. The dependence can also be described by a power law of the same type as Eq. 1, that is

$$t_F = A_F \cdot F^{n_F} \tag{2}$$

with negative values of power $n_F = -29$ at 623 K and -21 at 723 K. The absolute values of n_F are lower than the values for the hot-extruded material reported previously (-37 at 623 K and -33 at 723 K [28]). The times to fracture in the ECAP material are shorter than in the hot-extruded material, though the relative difference is smaller than in the previous case of the deflection rate. Assuming the same value of the power n_F in both materials, the time to facture is about 43 times shorter at 623 K and 14 times shorter at 723 K. The ratio at 723 K should be taken with caution since its force dependence has to be admitted.

The deflections observed at fracture, δ_F, are given for both materials in Fig. 4. The dependence can hardly be described analytically. The difference in fracture deflection between the HE and ECAP materials is negligible. The observed values range between 0.6 and 0.9 mm. These deflections are substantially lower than the fracture deflections found in heat-resistant steels [32, 33]. This fact corresponds to the low-creep ductility of this composite [34].

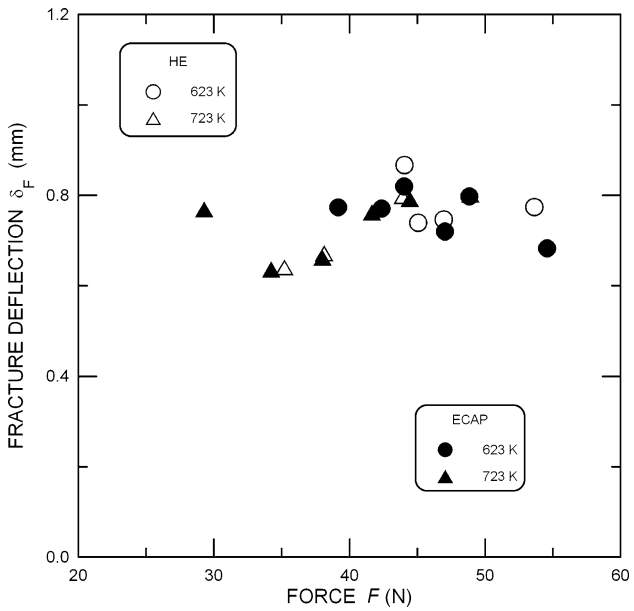

Fig. 4 Force dependence of the fracture deflection

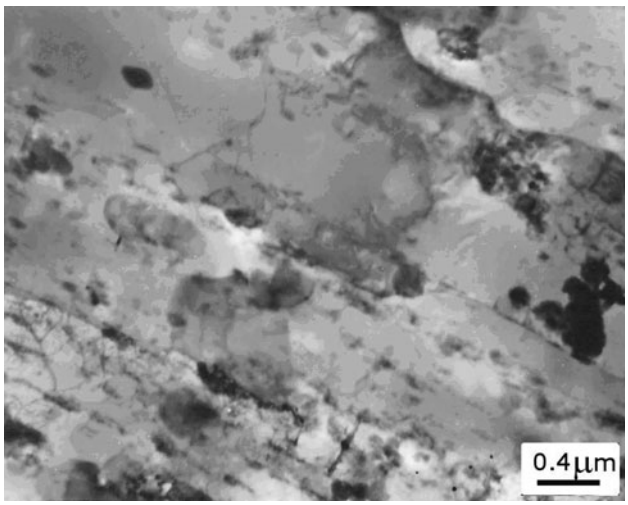

Fig. 5 The microstructure of the hot-extruded material

The microstructure of the hot-extruded material was fine-grained with a mean grain size of about 0.6 μm. The Al_4C_3 particles were distributed in parallel rows as a consequence of extrusion, cf. Fig. 5. In addition to the carbides, the material also contained Al_2O_3 particles. Essentially, they were the remnants of the oxide shells of the original matrix powder and/or shells formed during reaction milling. In fact, three distinctive groups of particles can be observed: (i) small Al_4C_3 particles, identified by TEM, with a mean size approximately of 30 nm, which made up to 70% of the dispersoid volume fraction; (ii) large Al_4C_3 particles with a mean size between 1 and 2 μm, identified by scanning electron microscopy and on metallographic micrographs and (iii) large Al_2O_3 particles with the mean size of 1 μm, found on metallographic micrographs and identified by scanning electron microscopy. Morphologically, Al_4C_3 particles are elongated, and Al_2O_3 particles are spherical. The material after ECAP is on the border of nanostructured materials. The TEM micrographs (Fig. 6) showed that the mean grain size was 100–200 nm; dislocations were present in nanograins, but mostly on the boundaries.

Discussion

The high values of the force exponent n_F in the HE material were rationalized [28] by means of the threshold concept [35]. The existence of a threshold force can also be expected in the present results for the ECAP material. The threshold force was determined by plotting $\dot{\delta}^{1/n}$ against the applied force F on linear axes (cf. Fig. 7). The value $n = 5$ was chosen in agreement with a previous article [28]. The estimated values of the threshold force are given in Table 1. The threshold force is about 5 N greater in the HE than in the ECAP material.

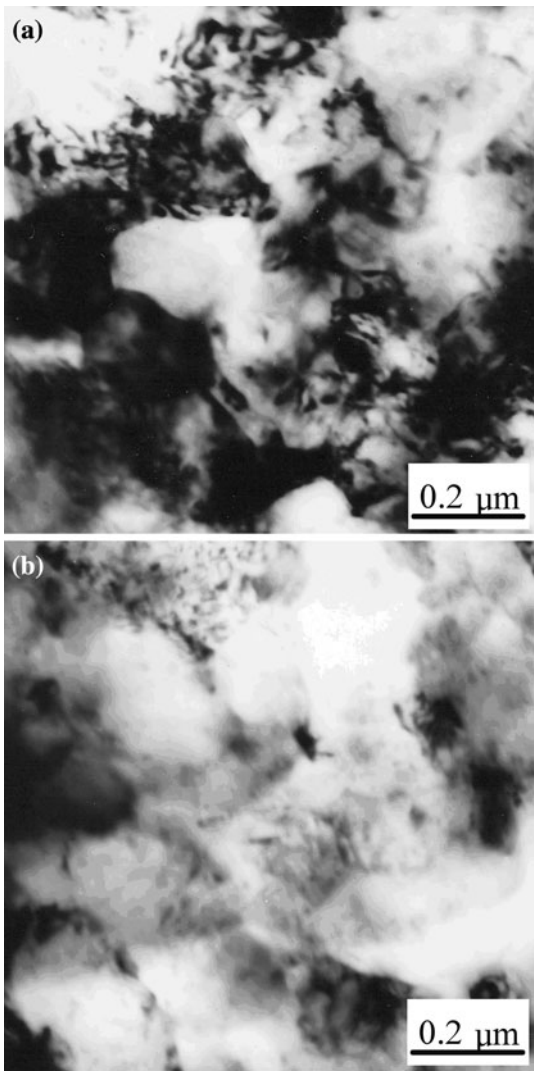

Fig. 6 The microstructure of the material after ECAP

It should be noted that the dependences in Fig. 7 differ in the HE and ECAP materials not only in terms of the value of the threshold force but also in terms of the values of their slopes. This can be explained by the following argument: the strain rate controlled by grain boundary processes can be generally [35, 36] described as

$$\dot{\varepsilon} = \frac{A_C D_{gb} G b}{kT}\left(\frac{b}{d}\right)^2\left(\frac{\sigma - \sigma_0}{G}\right)^n, \quad (3)$$

where A_C is a dimensionless constant, D_{gb} the coefficient of grain boundary diffusion, G the shear modulus, b the Burgers vector length, k the Boltzmann constant, T the absolute temperature, d the grain size, σ the applied stress and σ_0 the threshold stress. We can apply Eq. 3 to the SP results by substituting the strain rate by the deflection rate and the stresses by the respective forces and respecting the dimensionless form:

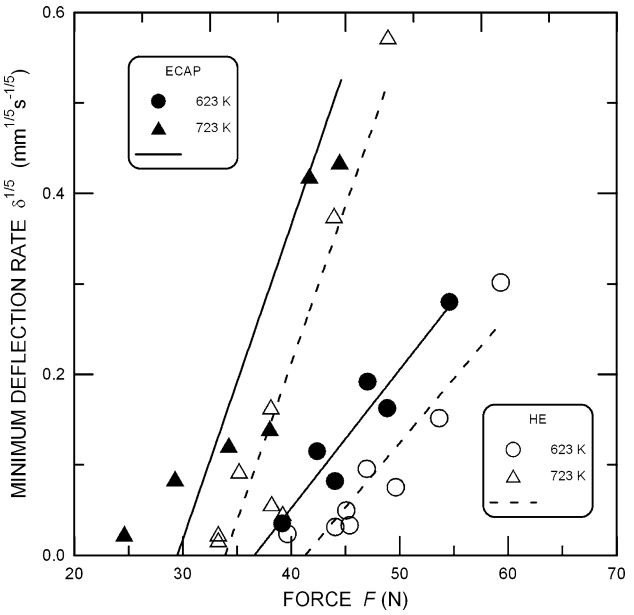

Fig. 7 Relation between $\dot{\delta}^{1/n}$ and the force for the true exponent $n = 5$

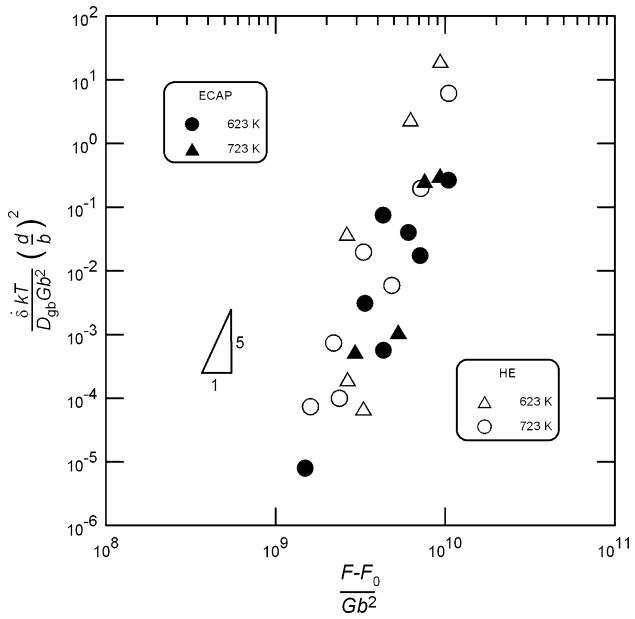

Fig. 8 Relation between normalized deflection rate and normalized effective force

Table 1 Estimated threshold force in HE and ECAP materials, respectively

Material	Temperature (K)	Threshold force (N)
HE	623	41.3
HE	723	33.9
ECAP	623	36.6
ECAP	723	29.5

$$\dot{\delta} = \frac{A_{SP} D_{gb} G b^2}{kT} \left(\frac{b}{d}\right)^2 \left(\frac{F - F_0}{Gb^2}\right)^n. \quad (4)$$

The slopes for the ECAP and HE materials in Fig. 7 should then be related as:

$$\frac{\frac{d\dot{\delta}^{1/n}_{ECAP}}{dF}}{\frac{d\dot{\delta}^{1/n}_{HE}}{dF}} = \left(\frac{d_{HE}}{d_{ECAP}}\right)^{2/n}. \quad (5)$$

The left-hand side of this equation as estimated from Fig. 7 is equal to 2.44 at 623 K and 2.27 at 723 K, and the right-hand side, as calculated from microscopic grain-size data, ranges from 1.55 to 2.05. Taking into account the uncertainties of both quantities, the agreement is quite plausible. We can further verify the above suggestion by plotting the normalized deflection rate $\frac{\dot{\delta} kT}{D_{gb} Gb^2}\left(\frac{d}{b}\right)^2$ versus the normalized effective force $\frac{F-F_0}{Gb^2}$; Fig. 8. For calculations, the following values of constants are applied: $b = 0.286$ nm, $G = 29{,}500 - 13.6 * T$ MPa and $wD_{gb} = 5 * 10^{-14} * \exp(-84{,}000/(RT))$ m^3 s^{-1} (w is the grain boundary width, $w = 0.5$ nm, and R is the universal gas constant) [29]. The mean value of grain size $d = 150$ nm of ECAP material was used and the data with negative value of the difference of applied force F and calculated threshold force F_0 were omitted. It is evident from Fig. 8 that the SP data for the HE and ECAP materials for both temperatures essentially superimpose. It indicates the importance of grain boundary processes in the control of the deformation mechanism. The main deformation mechanism can be the grain boundary sliding, which activates dislocation glide in the grain interiors. Both processes are inhibited by the presence of dispersed particles. A relative occupation of boundaries by particles is lower in the ECAP material, and it results in lower values of the threshold stress.

The stability of fine-grained microstructures in pure metals and single-phase solid solutions at elevated temperatures is usually not sufficient. The advantageous mechanical properties that are achieved by ECAP process are lost through grain growth when the material is heated. This is obviously not the case in the present composite due to the existence of second-phase particles that effectively retard the grain growth even at temperature of 723 K.

Conclusions

(1) The SP tests of a mechanically alloyed Al composite with a superimposed ECAP procedure were performed in the constant force regime at elevated temperatures. The force dependencies of the minimum deflection rate and of the time to fracture are qualitatively

comparable with the analogical dependences of the hot-extruded material.

(2) The ECAP does not improve the observed creep resistance. This can be attributed to smaller grain sizes as compared to hot-extruded material. The reduction of force leading to the same deflection rate is not very significant.

(3) The force dependence of the minimum deflection rate can be described in terms of the threshold force concept. The threshold force in the ECAP material is about 5 N weaker than in the HE material.

(4) The difference observed in the slopes of $\dot{\delta}^{1/n}$ versus force F in the HE and ECAP materials can be explained on the basis of the different grain sizes in both materials.

Acknowledgements This paper is based on work supported by the Academy of Sciences of the Czech Republic under Grant 1QS200410502 and by the grant agency VEGA, Slovak Republic within the project 2/5142/25. Special thanks are due to Prof. Dr. Gerhard Jangg, Dr. h.c. (formerly of Vienna University of Technology, Vienna, Austria) for providing the experimental material.

References

1. Clyne TW, Withers PJ (1993) An introduction to metal matrix composites. Cambridge University Press, Cambridge
2. Segal VM (1999) Mater Sci Eng A271:322
3. Lowe TC, Valiev RZ (2000) JOM J Min Met Mater Soc 52:27
4. Furukawa M, Horita Z, Nemoto M, Langdon TG (2001) J Mater Sci 36:2835. doi:10.1023/A:1017932417043
5. Valiev RZ, Langdon TG (2006) Prog Mater Sci 51:881
6. Nakashima K, Horita Z, Nemoto M, Langdon TG (1998) Acta Mater 46:1589
7. Huang WH, Chang L, Kao PW, Chang CP (2001) Mater Sci Eng A307:113
8. Semiatin SL, Delo DP, Shell EB (2000) Acta Mater 48:1841
9. Berbon PB, Furukawa M, Horita Z, Nemoto M, Langdon TG (1999) Met Mater Trans 30A:1989
10. Yamaguchi D, Horita Z, Nemoto M, Langdon TG (1999) Scr Mater 41:791
11. Yamashita A, Yamaguchi D, Horita Z, Langdon TG (2000) Mater Sci Eng A287:100
12. Mabuchi M, Higashi K (1998) J Mater Sci Lett 17:215
13. Furukawa M, Horita Z, Nemoto M, Valiev RZ, Langdon TG (1996) Mater Charact 37:277
14. Shan A, Moon IG, Ko HS, Park JW (1999) Scr Mater 41:353
15. Kawasaki M, Sklenička V, Langdon TG (2010) J Mater Sci 45:271. doi:10.1007/s10853-009-3975-9
16. Wu SD, Wang ZG, Jiang CB, Li GY, Alexandrov IV, Valiev RZ (2003) Scr Mater 48:1605
17. Stolyarov VV, Zhu YT, Alexandrov IV, Lowe TC, Valiev RZ (2003) Mater Sci Eng A343:43
18. Lapovok R, Tomus D, Mang J, Estrin Y, Lowe TC (2009) Acta Mater 57:2909
19. Figueiredo RB, Cetlin PR, Langdon TG (2007) Acta Mater 55:4769
20. Figueiredo RB, Langdon TG (2008) J Mater Sci 43:7366. doi:10.1007/s10853-008-2846-0
21. Valiev RZ, Islamgaliev RK, Kuzmina NF, Li Y, Langdon TG (1999) Scr Mater 40:117
22. Li Y, Langdon TG (2000) J Mater Sci 35:1201. doi:10.1023/A:1004740504619
23. Kawasaki M, Huang Y, Xu Ch, Furukawa M, Horita Z, Langdon TG (2005) Mater Sci Eng A410–411:402
24. Ramu G, Bauri R (2009) Mater Des 30:3554
25. Lucas GE (1990) Met Trans 21A:1105
26. Baik JM, Kameda J, Buck O (1983) Scr Met 17:1443
27. Evans M, Wang D (2008) J Mater Sci 43:1825. doi:10.1007/s10853-007-2388-x
28. Dobeš F, Milička K, Besterci M (2007) High Temp Mater Process 6:193
29. Frost HJ, Ashby MF (1982) Deformation-mechanism maps. The plasticity and creep of metals and ceramics. Pergamon Press, Oxford
30. Besterci M (2006) Mater Des 27(5):416
31. Besterci M, Kohutek I, Sulleiova K, Saxl I (1999) J Mater Sci 34:1055. doi:10.1023/A:1004552213455
32. Ule B, Šustar T, Dobeš F, Milička K, Bicego V, Tettamanti S, Maile K, Schwarzkopf C, Whelan MP, Kozlowski RH, Klaput J (1999) Nucl Eng Des 192:1
33. Dobeš F, Milička K, Ule B, Šustar T, Bicego V, Tettamanti S, Kozlowski RH, Klaput J, Whelan MP, Maile K, Schwarzkopf C (1998) Eng Mech 5:157
34. Orlová A, Kuchařová K, Čadek J, Besterci M (1986) Kovové Mater 24:505
35. Li Y, Langdon TG (1999) Acta Mater 47:3395
36. Langdon TG (1994) Acta Met Mater 42:2437